

# 1

## Fractional Calculus and Anomalous Transport

We first present the essential concepts of fractional calculus that will form a proper mathematical language for understanding and modeling *anomalous transport* phenomena. There are different ways of motivating and introducing the subject. For instance as the following historical review suggests, fractional calculus was developed shortly after the advent of the standard integer-order calculus and for the purpose of generalizing the notion of classical differentiation and integration to any non-integer order. While this school of thought is mathematically interesting, we find the multi-scale link between the fractional calculus and probability theory particularly fascinating and insightful. Hence in this chapter, we will have a step-by-step generalization of the standard/normal transport (diffusion) model to a variety of anomalous transport models, governed by fractional differential operators at the macroscopic level in addition to their direct connection to their underlying anomalous stochastic processes, occurring at the microscopic scale.

We initially introduce the standard (normal) diffusion model that solves the probability density function of the stochastic Brownian motion/process, satisfying the normal scaling property. Our first generalization of the standard diffusion happens then through a new definition of the process increments, where they no longer are drawn from a normal (Gaussian) distribution, leading to  $\alpha$ -stable Lévy flights at the microscopic level and correspondingly an anomalous diffusion model with a *fractional Laplacian* at the macroscopic scale that forms the first anomalous transport model we present in our book. Next, we show how the Riemann–Liouville fractional derivatives emerge in another anomalous diffusion model corresponding to the asymmetric  $\alpha$ -stable Lévy flights at small scales. Subsequently, we introduce the notion of subdiffusion stochastic processes, in which the Caputo time-fractional derivative appears in the anomalous subdiffusion fractional model. Interestingly we combine the previous two cases, and construct *continuous-time random walks*,

where a space-time fractional diffusion model will solve the evolution of the probability density function of the stochastic process. In the rest of the chapter, we motivate and introduce many other types of fractional derivatives that will code more complexity and variability at micro-to-macroscopic scales, including fractional material derivatives, time-variable diffusivity for the fractional Brownian motion, tempered/variable-order/distributed-order/vector fractional calculus, etc. We will end this chapter with a clarifying discussion on the notion of global versus local numerical methods for solving fractional differential equations, and why we are mainly regarding global (i.e., spectral and spectral element methods) for solving an array of fractional models for anomalous transport phenomena throughout the present book.

## 1.1 A Short Historical Review

The theory of classical *integer-order* calculus was independently developed by Isaac Newton and Gottfried Wilhelm Leibniz in seventeenth-century Europe, while its initial notion and basic ideas had in fact appeared in ancient Egypt, Greece, then in China and the Middle East, and later on, in medieval Europe and in India. Yet the notion of *fractional calculus*, as a generalizing theory dealing with derivatives/integrals of any (real or complex) arbitrary orders, first appeared in a letter written to Guillaume de l'Hôpital by Gottfried Wilhelm Leibniz in 1695, which can be marked as the birth certificate of fractional calculus. Shortly after the advent of standard calculus, Leibniz himself wrote to one of the Bernoulli brothers describing the similarity between the binomial theorem and the Leibniz rule for the fractional derivative of a product of two functions, breaking new mathematical ground for the development of a *non-integer order* theory. Subsequently, the term “fractional calculus” was officially introduced in Niels Henrik Abel’s early work in Abel (1823), where all the fundamental elements of such generalizing calculus were constructed. Interestingly and independently, the foundations of the subject were laid by Liouville (1832a,b), where along his line of thought, Bernhard Riemann established a rather more solid approach to construct the fractional operators by introducing new crucial mathematical building blocks. It should be noted that in his work (which was published after his death in Riemann (1876)), Riemann faced some serious technical problems with the notion of “an arbitrary function of integration” (issues like the constant of integration in evaluation of standard indefinite integrals, or anti-derivatives, or primitive functions). Consequently, he could not continue this approach. It was in fact A. V. Letnikov, a Russian mathematician, who later obtained the first rigorous and comprehensive

construction of the theory of the fractional integro-differentiation, which was later called the “*Riemann–Liouville integral and derivative*”. An extended description of his results can be found in Letnikov and Chernykh (2011).

## 1.2 Why Anomalous Transport and Fractional Modeling?

The classical calculus leads to the formulation of differential/integral/integro-differential operators, all integer orders being associated with their underlying conventional statistical physics. However such models cannot fully describe/predict the realistic nonlocal and complex nature of the *anomalous transport* phenomena due to their inherently local character in space-time. Nature is abundant with such processes, in which for instance a cloud of particles spreads in a different manner from traditional diffusion. This class of physical phenomena is characterized by fascinating processes that exhibit non-Markovian (long-range memory) effects, non-Fickian (nonlocal in space) interactions, non-ergodic statistics, and non-equilibrium dynamics. The phenomena of anomalous transport have been observed in a wide variety of complex, multi-scale, and multi-physics systems such as: *sub-/superdiffusion in subsurface transport, kinetic plasma turbulence, aging polymers, glassy materials, in addition to amorphous semiconductors, biological cells, heterogeneous tissues, and fractal disordered media*, see e.g., Klages et al. (2008) and references therein. From the scientific point of view, better understanding and effective exploiting of anomalous transport phenomena via fractional operators will continue to improve and perhaps transform our perspectives towards future discoveries.

## 1.3 Anomalous Transport and Stochastic Processes

Fractional calculus is a natural mathematical language for representing anomalous transport from *micro-to-macro* phenomena. In fact, fractional calculus establishes an interconnecting bridge at the interface between statistical physics, differential equations, and probability theory. Therefore, we find it effective to begin by introducing and classifying the most commonly used types of fractional-order differential operators in the context of *diffusion models based on random walks*. In this regard, and for simplicity, we restrict our discussion to one spatial dimension except for a few remarks, in which the extension to higher dimensions is touched upon. For other pedagogical reasons, we aim to describe the underlying stochastic processes in terms of their discretizations, thinking of them as sequences of random variables  $X_{n\Delta t}$ ,

defined as the cumulative sum of jumps at time  $n\Delta t$ , where  $\Delta t > 0$  denotes the time-step of the random walker and the integer  $n$  represents the number index of the jump. We will show how fractional partial differential equations (FPDEs) govern the statistical properties of *continuous-time* random walks, which are appropriate scaling (or long-time) limits of the discrete random walks.

Before we begin our introduction to the stochastic processes, we provide a summary of symbols used in Chapter 1, in addition to their descriptions, and the referral to their definitions or first appearance in Table 1.1.

### 1.3.1 Standard (Normal) Diffusion

The connection between Brownian motion  $B_t$  and the standard diffusion model was studied in seminal works by Louis Bachelier (1900) and Albert Einstein (1905). The diffusion equation is posed in

$$\begin{cases} \frac{\partial u}{\partial t}(x, t) = k^2 \Delta u(x, t), & x \in \mathbb{R}, \quad t > 0, \\ u(x, t = 0) = u_0(x), & x \in \mathbb{R}, \end{cases} \quad (1.3.1)$$

as a mixed initial/boundary value problem in which  $k^2 > 0$  is the diffusion coefficient and  $\Delta u = \partial^2 u / \partial x^2$  denotes the standard (integer-order) Laplacian. Brownian motion  $B_t$  is a continuous-time stochastic process defined for  $t \geq 0$ , whose discretized version using the time-step  $\Delta t$  has the property that  $B_{t=0} = 0$  and

$$B_{t+\Delta t} = B_t + \Delta B; \quad \Delta B \sim \mathcal{N}(\mu = 0, \sigma = k\sqrt{\Delta t}), \quad (1.3.2)$$

where  $\Delta B$ 's denote independent and identically distributed (i.i.d.) increments. The notation  $\sim$  indicates that the increment  $\Delta B$  at each time-step of  $\Delta t$  is drawn from a normal distribution  $\mathcal{N}(0, k\sqrt{\Delta t})$  with mean  $\mu = 0$  and standard deviation  $\sigma = k\sqrt{\Delta t}$ , where the corresponding normal probability density function (PDF) is explicitly given by

$$p_{\mathcal{N}}(x; \mu, \sigma) = \frac{1}{\sigma\sqrt{2\pi}} e^{-\frac{1}{2}\left(\frac{x-\mu}{\sigma}\right)^2}. \quad (1.3.3)$$

The rule (1.3.2) for sampling a path of  $B_t$  at times  $m\Delta t$ ,  $m = 0, 1, 2, \dots$ , is an example of a discrete stochastic differential equation (SDE), and is referred to as the *Euler–Maruyama* discretization of Brownian motion (Kloeden and Platen, 1992)<sup>1</sup>. The discrete process  $B_{m\Delta t}$  should be thought of as tracing

<sup>1</sup> Another frequently used discrete random walk that leads to Brownian motion simply involves steps of fixed length to the left or right with probability 1/2 each; see Lawler (2010). In the

Table 1.1. Symbols used in Chapter 1, their description, and the referral to their equation/section.

Symbol	Description	Equation/Section
$\frac{\partial}{\partial t}$	Partial derivative in time	(1.3.1)
$\Delta$	Laplacian	(1.3.1)
$\mathcal{N}(\mu, \sigma)$	Normal random variable	(1.3.2)
$B_t$	Brownian motion	(1.3.2)
$\langle \cdot \rangle$	Mean of a random variable	(1.3.4)
$\alpha$	Fractional order of spatial derivative	Sec. 1.3.2
$S_\alpha$	Stable random variable	Sec. 1.3.2
$f_\alpha$	Stable density function	(1.3.13)
$X_t^\alpha$	Stable Lévy walk	(1.3.15)
$(-\Delta)^{\alpha/2}$	Fractional negative Laplacian	(1.3.17)
$\Gamma$	Gamma function	(1.3.18)
$\mathcal{F}$	Fourier transform	(1.3.20)
${}^{\text{RL}}_a D_x^\alpha$	Left-sided Riemann–Liouville derivative	(1.3.24)
${}^{\text{RL}}_x D_b^\alpha$	Right-sided Riemann–Liouville derivative	(1.3.25)
$X_t^{\alpha,p}$	Asymmetric Lévy walk	(1.3.29)
$(-\Delta)_M^{\alpha/2}$	Directional fractional Laplacian	(1.3.32)
$\beta$	Fractional order of temporal derivative	Sec. 1.3.4
$\Psi_\beta$	Standard stable subordinator density function	(1.3.34)
$\mathcal{L}$	Laplace transform	(1.3.36)
$B_{\tau(t)}$	Brownian motion with waiting times	Sec. 1.3.4
${}_a^{\text{C}} D_t^\beta$	Caputo derivative	(1.3.40)
$E_\theta$	One-parameter Mittag-Leffler function $E_{\theta,1}$	(1.3.42)
$B_H(t)$	Fractional Brownian motion	(1.3.61)
$H$	Hurst index	(1.3.62)
$\mathbb{E}[B_H(t)B_H(s)]$	Covariance structure of a fractional Brownian motion	(1.3.64)
$\frac{\partial^{\alpha,\lambda}}{\partial x^\alpha}$	Tempered fractional derivative	(1.3.65)
$\mathfrak{L}^{\alpha(\cdot,\cdot)}$	Variable-order fractional Laplacian	(1.3.67)
${}_{-\infty}^{\text{RL}} D_t^{\alpha(\cdot,\cdot)}$	Variable-order left-sided Riemann–Liouville derivative	(1.3.68)
${}_{-\infty}^{\text{C}} D_t^{\alpha(\cdot,\cdot)}$	Variable-order left-sided Caputo fractional derivative	(1.3.69)
$D_{\mathcal{D}}^\beta$	Distributed-order fractional derivative	(1.3.70)
$\Phi \mathcal{H}(\mathbb{R})$	Distributed fractional Sobolev space on $\mathbb{R}$	(1.3.71)
$\mathcal{J}_M^{1-\beta}$	Meerschaert et al.’s fractional integral	(1.3.74)
$\nabla_M^\beta$	Meerschaert et al.’s fractional gradient	(1.3.75)
$\text{div}_M^\beta V$	Meerschaert et al.’s fractional divergence	(1.3.76)
$\text{curl}_M^\beta V$	Meerschaert et al.’s fractional curl	(1.3.77)
$\text{Grad}_W^\alpha$	Tarasov’s fractional gradient	(1.3.78)
$\text{Div}_W^\alpha$	Tarasov’s fractional divergence	(1.3.79)
$\text{Curl}_W^\alpha$	Tarasov’s fractional curl	(1.3.80)

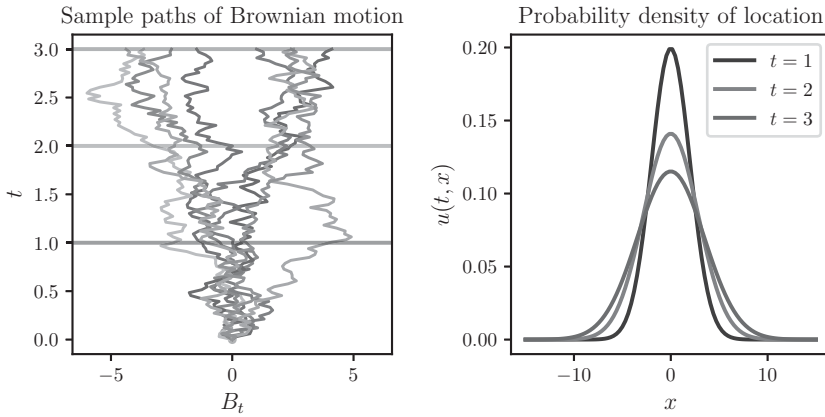


Figure 1.1 (Left) Eight independent sample paths of Brownian motion representing the path of a particle starting at the origin and stepping according to the rule (1.3.2). (Right) For  $t = 1, 2, 3$ , the probability density of the location of the particle, i.e., the fundamental solution to the classical heat equation (1.3.1). Source: Suzuki et al. (2023).

a path in  $\mathbb{R}$  of a particle undergoing “jumps” in a random direction at time intervals of size  $\Delta t$ . At each time  $t$ , the position  $B_t$  of the particle is a *random variable*. It can be shown that the paths of the continuous-time process  $B_t$  are almost surely continuous in time (Revuz and Yor, 2013). From (1.3.2) and the central limit theorem (CLT), it follows that Brownian motion satisfies the *linear scaling* property (in time), that is,

$$\langle B_t^2 \rangle = 2k^2 t, \quad (1.3.4)$$

where the left-hand side denotes the *variance* of the random variable  $B_t$ . Given an initial PDF of particles  $u_0(x)$  in  $\mathbb{R}$  at  $t = 0$ , which subsequently undergo Brownian motion, *the corresponding PDF of the cloud of particles in  $\mathbb{R}$  at each instance, i.e.,  $u(x, t)$ , is governed by (1.3.1)*. In other words, diffusing particles (random walkers) described at a *microscopic scale* by Brownian motion, i.e., by (1.3.2) in discrete time, have their PDF in space – a *macroscopic property* – governed by the diffusion (heat) equation (Meerschaert and Sikorskii, 2011, Section 1.1). This is illustrated in Figure 1.1.

The consistency between this macroscopic description and the microscopic model is illustrated by scaling properties. A necessary property of such a Brownian motion model is the second-moment condition (1.3.4), which states that on average, particles travel a distance  $k\sqrt{t}$  from their initial position after

long-time limit, all such discrete walks that draw increments from a finite-variance distribution lead to Brownian motion, due to the central limit theorem (Zaburdaev et al., 2015)

time  $t$ . This is reflected by the fact that the solution of (1.3.1) with initial condition  $u_0(x) = \delta(x)$ , being the Dirac delta function, is

$$u(x, t) = \frac{1}{\sqrt{4\pi t}} e^{-x^2/4k^2t}, \tag{1.3.5}$$

which is the normal density (1.3.3) with standard deviation  $k\sqrt{t}$ . Note that this solution has the property

$$u(x, t_2) = \left(\frac{t_2}{t_1}\right)^{-1/2} u\left(\frac{x}{(t_2/t_1)^{-1/2}}, t_1\right), \quad t_2 > t_1 > 0. \tag{1.3.6}$$

Thus, the distribution of a plume of particles in this diffusion model spreads out as  $(t_2/t_1)^{1/2}$  as time elapses from  $t_1$  to  $t_2$ , consistent with (1.3.4). The model for normal diffusion reviewed here is also referred to as *Fickian* diffusion. The heat equation (1.3.1) can be derived from the mass conservation with flux term  $J$ ,

$$\frac{\partial u}{\partial t} + \frac{\partial J}{\partial x} = 0 \tag{1.3.7}$$

under Fick’s law  $J = \nabla u$ . As discussed by Schumer et al. (2001), the fractional diffusion equations we introduce below follow from mass conservation with non-Fickian fluxes.

### 1.3.2 $\alpha$ -Stable Lévy Flights and Fractional Laplacian

There are important physical systems that exhibit diffusive behavior but do not satisfy the scaling property (1.3.4) (Klafter and Sokolov, 2005). This type of diffusion is referred to as *anomalous diffusion* as it cannot be adequately described by (1.3.2) with normally distributed increments. We need to develop a microscopic model that generalizes Brownian motion  $B_t$ , and a corresponding macroscopic model that generalizes the diffusion equation (1.3.1).

The first model we propose remains in the framework of a discrete SDE with (i.i.d.) increments,

$$X_{t+\Delta t} = X_t + \Delta X, \quad X_0 = 0, \tag{1.3.8}$$

but the increments  $\Delta X$  are no longer drawn from a normal distribution. It follows from the central limit theorem (CLT) that the only way to obtain a microscopic model in this framework that is statistically distinct from  $B_t$ , i.e., not equivalent in distribution, is to draw step sizes from a PDF with *infinite* variance (Zaburdaev et al., 2015; Meerschaert and Sikorskii, 2011).

We introduce the isotropic  $\alpha$ -stable random variable  $S_\alpha(\gamma, \sigma, \mu)$ . This family of random variables is defined by their *characteristic function*, defined

below<sup>2</sup>. For a general random variable  $X$ , the characteristic function  $\varphi_X$  is related to the PDF  $p_X$  by

$$\varphi_X(\xi) = \int e^{i\xi x} p_X(x) dx = \mathbb{E}[e^{i\xi x}], \quad (1.3.9)$$

being the mathematical expectation of the exponential function  $e^{i\xi x}$ . For instance, the characteristic function of the normal random variable is  $e^{i\xi\mu - \sigma^2\xi^2/2}$ . Moreover a straightforward calculation reveals that the  $\alpha$ -stable random variable has the following characteristic function

$$\varphi_\alpha(\xi; \gamma, \sigma, \mu) = e^{i\xi\mu - |\sigma\xi|^\alpha(1-i\gamma \operatorname{sgn}(\xi) \Phi)}, \quad (1.3.10)$$

where

$$\Phi = \begin{cases} \tan\left(\frac{\pi\alpha}{2}\right), & \text{if } \alpha \neq 1, \\ -\frac{2}{\pi} \log(|\sigma\xi|), & \text{otherwise.} \end{cases} \quad (1.3.11)$$

The parameter  $\alpha \in (0, 2]$  is referred to as the *stability parameter* of the distribution,  $\mu \in \mathbb{R}$  as the center of distribution, in addition,  $\gamma \in [-1, 1]$  denotes the skewness, and  $\sigma \in (0, \infty)$  represents the scale. The *isotropic* or *symmetric*  $\alpha$ -stable distribution  $S_\alpha(\gamma = 0, \sigma, \mu = 0)$  therefore has the characteristic function

$$\varphi_\alpha(\xi; \gamma = 0, \sigma, \mu = 0) = e^{-\sigma|\xi|^\alpha}, \quad (1.3.12)$$

generalizing the characteristic function of the normal distribution with mean  $\mu = 0$  and standard deviation  $\sigma/\sqrt{2}$  and reducing to it when  $\alpha = 2$ . By the Fourier inversion theorem, the PDF of  $S_\alpha(\gamma, \sigma, \mu)$  can be written

$$f_\alpha(x; \gamma, \sigma, \mu) = \frac{1}{2\pi} \int e^{-i\xi x} \varphi_\alpha(\xi; \gamma, \sigma, \mu) d\xi, \quad (1.3.13)$$

In general, the  $\alpha$ -stable density does not admit a closed-form expression<sup>3</sup>, but in the symmetric case where  $\gamma = \mu = 0$ , it has the property that

$$f_\alpha(x; \gamma = 0, \sigma, \mu = 0) \sim \frac{1}{|\sigma x|^{1+\alpha}} \quad \text{for large } x, \quad 0 < \alpha < 2, \quad (1.3.14)$$

as discussed in, e.g., Cont and Tankov (2003) or Nolan (2020). In other words, the density exhibits *power-law* (also called *Paretian*) tails. This is in contrast to the rapidly decaying square-exponential tails of the normal distribution. In

<sup>2</sup> Several parametrizations of the  $\alpha$ -stable characteristic function exist. The parametrization (1.3.10) is due to Samorodnitsky and Taquq (1994). See Nolan (1998, 2020) for discussions of alternate forms.

<sup>3</sup> Special cases are  $\alpha = 2$  corresponding to the normal distribution,  $\alpha = 1$  and  $\gamma = 0$  corresponding to the Cauchy distribution, and  $\alpha = 1/2$  and  $\gamma = 1$  corresponding to the Lévy distribution.

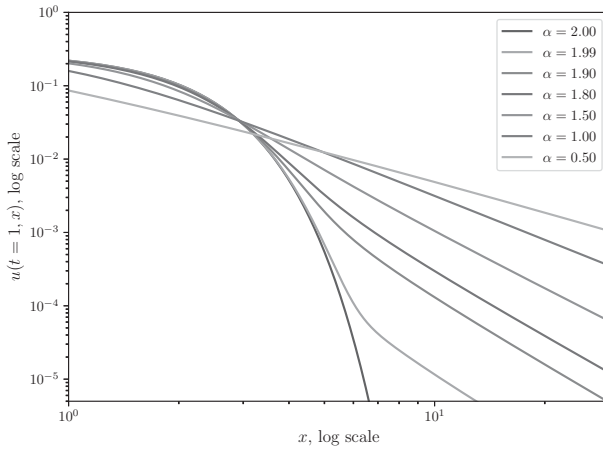


Figure 1.2 A plot of the  $\alpha$ -stable densities in a log-log scale that illustrates the tail behavior asserted in (1.3.14). While  $\alpha$ -stable densities do not have a closed form expression for all  $x$ , their simple, asymptotic inverse power-law behavior is an important heuristic. Source: Suzuki et al. (2023).

many settings, such tails are informally referred to as being examples of heavy tails or fat tails (Adler et al., 1998; Haas and Pigorsch, 2009), see Figure 1.2.

Using the isotropic distribution given above, we introduce the isotropic  $\alpha$ -stable Lévy flight  $X_t^\alpha$  by providing the corresponding discrete stochastic process. This is given for  $t = k\Delta t$  with integer  $k$  by  $X_0^\alpha = 0$  and the rule (Meerschaert and Sikorskii, 2011)

$$X_{t+\Delta t}^\alpha = X_t^\alpha + \Delta X^\alpha; \quad \Delta X^\alpha \sim S_\alpha(\gamma = 0, \sigma = k(\Delta t)^{1/\alpha}, \mu = 0). \quad (1.3.15)$$

The continuous-time stochastic process  $X_t^\alpha$  for  $t \geq 0$  can be thought of as a scaling limit as  $\Delta t \rightarrow 0$  of the above random walk, and enjoys several theoretical properties such as stability and an extended central limit theorem (Meerschaert and Scheffler, 2001). However, it also has the property that for  $\alpha < 2$ , the paths of  $X_t^\alpha$  are almost surely *discontinuous*, in contrast to Brownian motion; hence, the name Lévy “flight”.

Given an initial distribution  $u_0(x)$  of particles in  $\mathbb{R}$  which undergo  $\alpha$ -stable Lévy flight, the evolution of the distribution  $u(x, t)$  for  $t > 0$  is governed by the *space-fractional* diffusion equation (Meerschaert and Sikorskii, 2011, Section 1.2)

$$\begin{aligned} \frac{\partial u}{\partial t}(x, t) &= -k^\alpha(-\Delta)^{\alpha/2}u(x, t), \\ u(x, 0) &= u_0(x), \end{aligned} \quad (1.3.16)$$

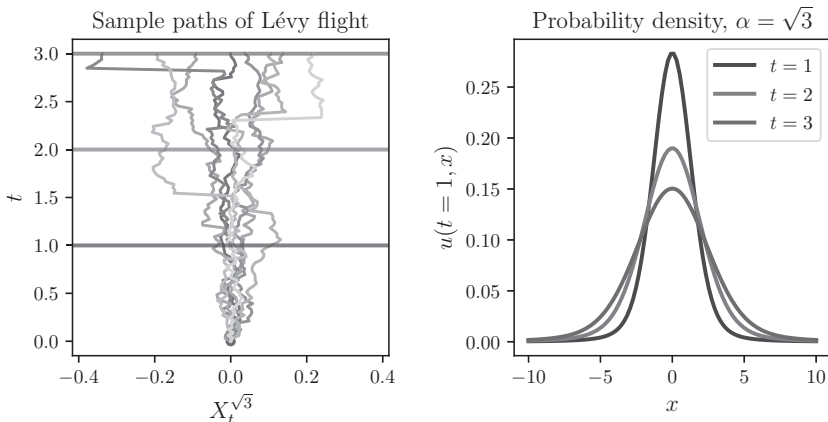


Figure 1.3 (Left) Eight independent sample paths of symmetric  $\alpha$ -stable Lévy flight with  $\alpha = \sqrt{3}$  representing the path of a particle starting at the origin and stepping according to the rule (1.3.15). (Right) For  $t = 1, 2, 3$ , the probability density of the location of the particle given by (1.3.13), i.e., the fundamental solution to the fractional diffusion equation (1.3.16). Compared to Figure 1.1, note that despite some qualitative similarity between the shapes of the density functions, the presence of long jumps signifies a striking difference between the paths of a particle undergoing Lévy flight versus Brownian motion. Source: Suzuki et al. (2023).

as illustrated in Figure 1.3. The fractional power of the negative Laplacian  $(-\Delta)^{\alpha/2}$  is defined for  $0 < \alpha < 2$  and for any dimension  $d$  as

$$(-\Delta)^{\alpha/2}u(x) = C_{d,\alpha} \text{p.v.} \int_{\mathbb{R}^d} \frac{u(x) - u(y)}{|x - y|^{d+\alpha}} dy, \quad x \in \mathbb{R}^d, \tag{1.3.17}$$

with

$$C_{d,\alpha} = \frac{4^{\alpha/2} \Gamma(\alpha/2 + \frac{d}{2})}{\pi^{d/2} |\Gamma(-\alpha/2)|}; \tag{1.3.18}$$

see Lischke et al. (2020), where “p.v.” denotes the principal value of the singular integral. We have defined this operator in any dimension for future reference, although our present discussion is only restricted to the case  $d = 1$ . Perhaps the simplest characterization of the fractional Laplacian is the Fourier representation,

$$\mathcal{F}[(-\Delta)^{\alpha/2}u](\xi) = |\xi|^\alpha \mathcal{F}[u](\xi), \tag{1.3.19}$$

where the Fourier transform is

$$\mathcal{F}[u](\xi) = \int e^{-i\xi x} u(x) dx. \tag{1.3.20}$$

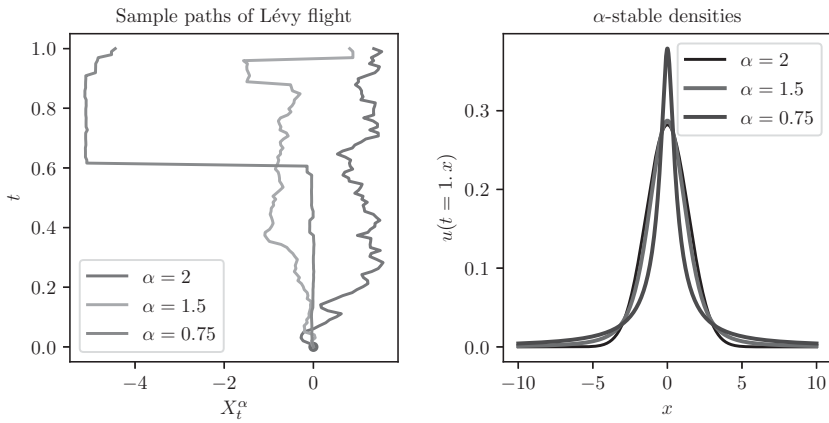


Figure 1.4 The seemingly innocuous heavy tails of the  $\alpha$ -stable density, signifying non-vanishing probability of long jumps, are responsible for the striking properties of  $\alpha$ -stable Lévy flights. As  $\alpha$  decreases from 2, more mass in the middle region of the density is lost and is transferred towards the tails and the center, so that the relative probability of very small movements and very long movements increases (right). This is evident in the sample paths of the process (left). Source: Suzuki et al. (2023).

The simplest case of (1.3.16) is the initial condition  $u_0(x) = \delta(x)$ , in which case the solution is

$$u(x, t) = f_\alpha(x; \gamma = 0, \sigma = kt^{1/\alpha}, \mu = 0). \tag{1.3.21}$$

This is known as the fundamental solution. Although this solution cannot be written in closed form, it satisfies

$$u(x, t_2) = \left(\frac{t_2}{t_1}\right)^{-1/\alpha} u\left(\frac{x}{(t_2/t_1)^{-1/\alpha}}, t_1\right), \quad t_2 > t_1 > 0, \tag{1.3.22}$$

as shown in Meerschaert and Sikorskii (2011, Section 1.2). This illustrates that a plume of particles undergoing isotropic  $\alpha$ -stable Lévy flight spreads by a factor of  $(t_2/t_1)^{1/\alpha}$  as time elapses from  $t_1$  to  $t_2$ , a faster rate when  $\alpha < 2$  than the normal rate  $t^{1/2}$ . Thus, the  $\alpha$ -stable Lévy flight is an example of *superdiffusion*. The dependence of the above solution as well as sample paths on  $\alpha$  is shown in Figure 1.4.

**Remark 1.1** Since  $\alpha > 0$ , the tail behavior of the isotropic  $\alpha$ -stable density implies that the second moment of  $X_t^\alpha$  diverges for  $\alpha < 2$ ,

$$\langle X_t^\alpha \rangle^2 = \infty, \quad 0 < \alpha < 2. \tag{1.3.23}$$

with the first moment (the mean) diverging also when  $\alpha \leq 1$  (Nolan, 2020; Zaburdaev et al., 2015). This implies that the variance of  $\alpha$ -stable motion is not a useful statistic for parametrizing  $\alpha$ -stable Lévy flight; it bears no useful relationship to  $\alpha$ . This aspect can be tackled in several ways, motivating the introduction of further fractional-order operators, such as tempered operators and fractional material derivatives.

While we will later provide a rather comprehensive description of fractional Laplacian in addition to its meaning and properties in Chapter 6, we briefly point out several important properties of the fractional Laplacian:

- (1)  $(-\Delta)^{\alpha/2}c = 0$ , for constant  $c$ .
- (2) The fractional Laplacian satisfies the *semigroup* property  $(-\Delta)^{\alpha/2}(-\Delta)^{\beta/2} = (-\Delta)^{(\alpha+\beta)/2}$  (Samko et al., 1993).
- (3) Unlike integer-order derivatives, the fractional Laplacian is indeed a *nonlocal* operator, i.e., the value of  $(-\Delta)^{\alpha/2}u(x)$  depends on the values of  $u$  in all of  $\mathbb{R}$  (or  $\mathbb{R}^d$ , for  $d > 1$ ). In contrast, the value of any integer-order derivative of  $u$  at  $x$  depends only on the values of  $u$  in an infinitesimal neighborhood of  $x$ .

### 1.3.3 The Riemann–Liouville Fractional Derivatives and Asymmetric $\alpha$ -Stable Lévy Flight

The fractional Laplacian (1.3.17) was introduced in the previous section as a symmetric or rotation invariant operator for describing the symmetric or isotropic  $\alpha$ -stable Lévy flight. This model involved a stability parameter  $0 < \alpha \leq 2$  allowing it to generalize normal diffusion, with the scale  $\sigma$  and center  $\mu$  playing similar roles as the standard deviation and mean of the normal distribution. However, the stable distribution also allows for a skewness parameter  $\gamma \in [-1, 1]$ , with  $\beta = 0$  in the symmetric case, which has no analogue in the normal distribution or for Brownian motion. This is due to the CLT, which states that the use of any finite-variance distribution for the i.i.d. increments  $\Delta X$  in (1.3.8), no matter how asymmetric, leads to  $X_t$  being normally distributed, so that the density is necessarily symmetric about the mean.

In this section, we introduce the one-sided Riemann–Liouville fractional derivatives as appropriate operators for modeling asymmetric  $\alpha$ -stable Lévy flights, which are defined by (1.3.15) with  $\Delta X^\alpha \sim S_\alpha(\gamma, \sigma = k(\Delta t)^{1/\alpha}, \mu = 0)$  for nonzero  $\beta$ . The left-sided and right-sided Riemann–Liouville derivatives in  $\mathbb{R}$  are defined, for  $n = \lceil \alpha \rceil$ , as

$${}^{\text{RL}}D_a^\alpha u(x) = \frac{1}{\Gamma(n - \alpha)} \left[ \frac{d^n}{dz^n} \int_a^z \frac{u(y)}{|z - y|^{\alpha-n+1}} dy \right]_{z=x}, \tag{1.3.24}$$

$${}^{\text{RL}}D_x^\alpha u(x) = \frac{(-1)^n}{\Gamma(n - \alpha)} \left[ \frac{d^n}{dz^n} \int_z^b \frac{u(y)}{|z - y|^{\alpha-n+1}} dy \right]_{z=x}. \tag{1.3.25}$$

The books of Podlubny (1999), Oldham and Spanier (1974), and Meerschaert and Sikorskii (2011) discussed these operators in detail. These derivatives are frequently used in models with  $a = -\infty$  and  $b = \infty$ . In connection with initial-value problems (IVPs), the left-sided Riemann–Liouville derivative in time,  ${}^{\text{RL}}D_0^\alpha u(t)$ , is sometimes used with  $a = 0$ . We have written the definitions (1.3.24) and (1.3.25) to avoid ambiguities in notation, and clearly show that substitution of the variable  $x$  occurs after integration and differentiation. An alternative approach is to define the Riemann–Liouville fractional integrals separately, as in the right-hand sides of (1.3.24) and (1.3.25); see Samko et al. (1993).

One quirk of the notation for Riemann–Liouville derivatives in (1.3.24) and (1.3.25) is the subtle writing of the upper and lower limits of integration  $[a, x]$  and  $[b, x]$ , respectively, as subscripts. While this is suggestive, the result is that the variable of evaluation  $x$  occurs twice in the notation for each operator. If these derivatives are evaluated at any fixed value of  $x$ , this value should be substituted in both locations; thus,  ${}^{\text{RL}}D_5^\alpha u(5)$  represents a valid evaluation of the derivatives, but  ${}^{\text{RL}}D_x^\alpha u(5)$  and  ${}^{\text{RL}}D_5^\alpha u(x)$  do not.

With  $a = -\infty$  and  $b = \infty$ , the Riemann–Liouville derivatives can be represented by the following Fourier representations

$$\mathcal{F} [ {}^{\text{RL}}D_{-\infty}^\alpha u ] (\xi) = (-i\xi)^\alpha \mathcal{F} [ u ] (\xi), \tag{1.3.26}$$

$$\mathcal{F} [ {}^{\text{RL}}D_x^\alpha u ] (\xi) = (i\xi)^\alpha \mathcal{F} [ u ] (\xi). \tag{1.3.27}$$

In one dimension, these can be used in the asymmetric diffusion model

$$\begin{aligned} \frac{\partial u}{\partial t}(x, t) &= \frac{-k^\alpha}{\cos(\pi\alpha/2)} \left[ p {}^{\text{RL}}D_{-\infty}^\alpha u(x, t) + (1 - p) {}^{\text{RL}}D_x^\alpha u(x, t) \right], \\ u(x, t = 0) &= u_0(x), \end{aligned} \tag{1.3.28}$$

which describes anomalous diffusion of independent particles. Here, the positions of each particle at time-steps of  $k\Delta t$  for integer  $k$  are governed by (1.3.8) with increments  $\Delta X$  being drawn from the *asymmetric*  $\alpha$ -stable distribution

$$\Delta X \sim S_\alpha(\gamma = 2p - 1, \sigma = k(\Delta t)^{1/\alpha}, \mu = 0). \tag{1.3.29}$$

The resulting random variable given by the sum of  $k$  increments is denoted by  $X_t^{\alpha,p}$ , for  $t = k\Delta t$ . Thus, the skewness ranges from  $\gamma = -1$  when  $p = 0$  to  $\gamma = 1$  when  $p = 1$ . The fundamental solution of (1.3.28) cf. (1.3.21) is

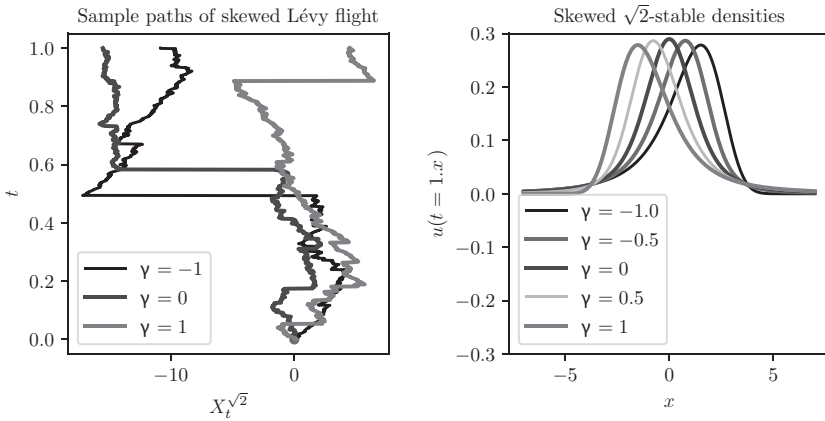


Figure 1.5  $\alpha$ -stable Lévy flights allow for asymmetric diffusion, which has no analogue within the classical diffusion framework. The  $\alpha$ -stable density (1.3.29) admits a skewness parameter  $\beta$ , ranging from  $-1$  to  $1$ , which can adjust the relative probability of long jumps in a given direction (*right*), a statistical property that is evident in the sample paths (*left*). Such models are governed by the fractional-order diffusion equation involving Riemann–Liouville derivatives, as in (1.3.28). Source: Suzuki et al. (2023).

$$u(x, t) = f_\alpha(x; \gamma = 2p - 1, \sigma = kt^{1/\alpha}, \mu). \tag{1.3.30}$$

Sample paths of the process  $X_t^{\alpha,p}$  are illustrated in Figure 1.5. Note that when  $p = 1/2$ , the distribution reverts to the symmetric  $\alpha$ -stable distribution, and it can be shown in this case that (1.3.28) reduces to (1.3.16); more specifically,

$$\frac{1}{\cos(\pi\alpha/2)} \left[ \frac{1}{2} \left( {}^{\text{RL}}D_x^\alpha u(x) \right) + \frac{1}{2} \left( {}^{\text{RL}}D_x^\alpha u(x) \right) \right] = (-\Delta)^{\alpha/2} u(x). \tag{1.3.31}$$

The Fourier representation (1.3.26) suggests that the left-sided Riemann–Liouville derivative  ${}^{\text{RL}}D_x^\alpha u$  should be thought of as a fractional power of the operator  $\partial/\partial x$ . However, the correspondence between (1.3.28) and (1.3.29) makes it clear that to obtain a complete description of  $\alpha$ -stable Lévy flights in one dimension necessitates two operators, a left-sided and a right-sided operator, which agree with one another when  $\alpha = 2$ . Our interest in these models lies in the fact that an extended CLT holds for processes with i.i.d. increments drawn from distributions with infinite variance, but for which the tails of the density function satisfy Pareto-type conditions as in (1.3.14). For such processes,  $\alpha$ -stable distributions play an analogous role to the normal distribution in the classical central limit theorem; unlike the classical theorem,

for full generality, skewed  $\alpha$ -stable distributions must be included in such a result. See Meerschaert and Scheffler (2001) or Meerschaert and Sikorskii (2011) for a treatment of these results.

We note that the Riemann–Liouville derivative can be utilized in dimensions  $d > 1$ . An anisotropic diffusion operator was introduced by Meerschaert et al. (1999) and Benson et al. (2000) as

$$\begin{aligned}
 -(-\Delta)_M^{\alpha/2} u(x) &= C_{\alpha,d} \int_{|\theta|=1} D_\theta^\alpha u(x) M(d\theta), & (1.3.32) \\
 C_{\alpha,d} &= \frac{\Gamma\left(\frac{1-\alpha}{2}\right) \Gamma\left(\frac{d+\alpha}{2}\right)}{2\pi^{\frac{1+d}{2}}},
 \end{aligned}$$

where  $M(d\theta)$  denotes a non-negative measure on the angle  $\theta$  in the unit sphere  $\{|\theta| = 1\}$  in  $\mathbb{R}^d$ , and the Riemann–Liouville directional derivative is given by

$$D_\theta^\alpha u(x) = {}_{-\infty}^{\text{RL}} D_t^\alpha v(t) \Big|_{t=0}, \quad \text{where } v(t) = u(x + t\theta).$$

Benson et al. (2000) showed that when the measure  $M$  is uniform, the operator (1.3.32) reduces to the fractional Laplacian (1.3.17). In higher dimensions and for general measures  $M$ , the operator (1.3.32) plays an analogous role to the operator in the right-hand side of (1.3.28), which is in fact a special case of it for  $d = 1$ . As such, it is used in models of anisotropic multivariate  $\alpha$ -stable Lévy diffusion.

### 1.3.4 Subdiffusion and Caputo Fractional Derivatives

The superdiffusive model introduced above, in which a plume of particles spreads out in space with rate  $t^{1/\alpha}$  for  $0 < \alpha < 2$ , raises the question of whether a process can be constructed which results in diffusion *slower* than the Brownian rate  $t^{1/2}$ . In this section, we introduce such a model, constructed as Brownian motion with random waiting times drawn from a skewed stable distribution, supported over positive real numbers with a power-law tail. Here, we step away from the framework of the SDE given by (1.3.8). Rather than being defined by a simple time-stepping scheme with i.i.d. increments, the paths of the process are defined by a transformation or *post-processing* of Brownian paths  $B_t$ .

We introduce Brownian motion with waiting times, denoted by  $B_{\tau(t)}$ . The intuition is that the particle paths traced out in space by a discretization of  $B_{\tau(t)}$  are paths of discretized Brownian motion  $B_t$ , but the particles wait at each point of the path for a random time drawn from the totally skewed stable distribution. The operational time  $\tau(t)$ , which introduces waiting and replaces linear time  $t$ , is an *inverse stable subordinator*. This is a stochastic process

in the variable  $t$ , although we write  $\tau(t)$  rather than using a subscript for typographical reasons. This process is constructed by first defining the *stable subordinator*  $D(t)$ , and defining  $\tau(t)$  to be the inverse process of  $D(\tau)$ <sup>4</sup>. Both  $D(t)$  and  $\tau(t)$  are nondecreasing processes with time. In terms of paths,  $\tau(t)$  arises from  $D(t)$  as

$$\tau(t) = \inf\{\tau \text{ such that } D(\tau) > t\}. \quad (1.3.33)$$

Intuitively,  $D(t)$  represents a cumulative waiting time process, keeping track of the total time waited by a particle throughout a path, while the inverse  $\tau(t)$  represents an operational time, i.e., the time spent traveling. The increments of  $D(t)$  represent the time waited at each location of a particle before the jump to the next location. More specifically,  $D(t)$  is a totally skewed  $\beta$ -stable Lévy process (1.3.29) with stability index  $\beta \in (0, 1)$ ,  $\gamma = 1$ , scale  $\sigma = \cos(\pi\beta/2)$ , and center  $\mu = 0$ ; see Meerschaert and Sikorskii (2011), Example 5.14. The construction of sample paths of  $B_{\tau(t)}$  is demonstrated in Figure 1.6. The resulting probability density function of  $D(t)$ ,

$$\psi_\beta(t) = f_\beta(t; \gamma = 1, \sigma = \cos(\pi\beta/2), \mu = 0) \quad (1.3.34)$$

for waiting times is supported in non-negative real numbers. Due to the non-negative support of the waiting time density, the characteristic function (1.3.10) yields the Laplace transform of the waiting time density as

$$\mathcal{L}[\psi_\beta](s) = e^{-s^\beta}, \quad (1.3.35)$$

where the Laplace transform is defined as

$$\mathcal{L}[u](s) = \int_0^\infty e^{-st} u(t) dt. \quad (1.3.36)$$

See Meerschaert and Sikorskii (2011), p. 108 and p. 156 for a discussion. The variance of the process  $B_{\tau(t)}$  is given by

$$\langle B_{\tau(t)} \rangle^2 = \frac{2}{\Gamma(\beta + 1)} t^\beta, \quad 0 < \beta < 1, \quad (1.3.37)$$

which is the desired subdiffusive property. Note that the finiteness of the variance does not imply that the normal CLT applies to  $B_{\tau(t)}$ , which is not equal in distribution to Brownian motion nor to any Lévy process. In fact,  $B_{\tau(t)}$  is not a Markov process.

<sup>4</sup> The definition of  $\tau$  in terms of  $D$  is an example of a right-continuous inverse of an increasing function. Paths of  $D$ , thought of as functions of  $t$ , are nondecreasing, so that each path of  $\tau$  constructed in this way is a continuous-from-the-right inverse of the parent path of  $D$  used to construct it.

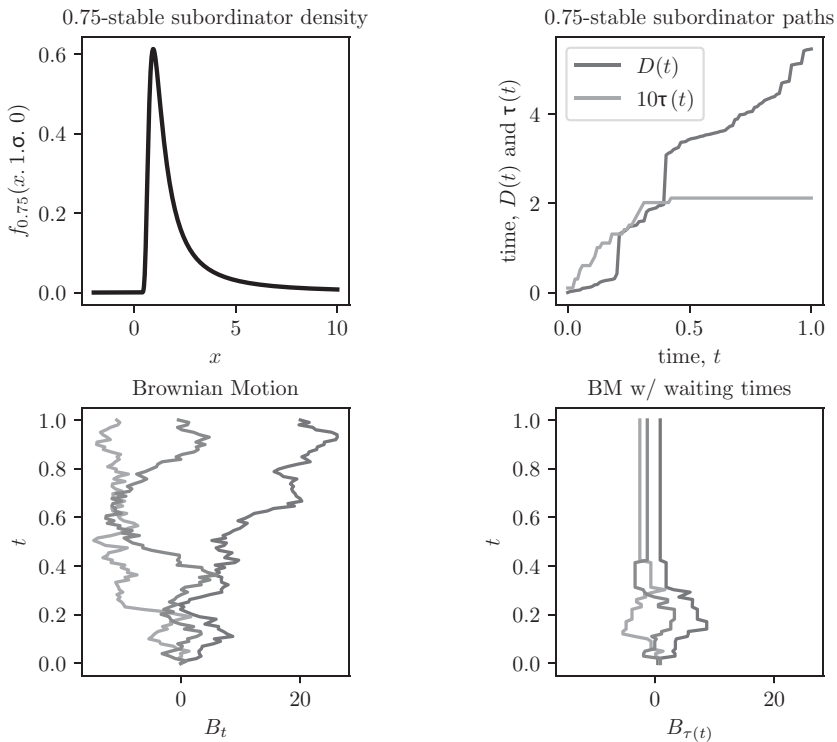


Figure 1.6 (Top left) Example of an  $\alpha$ -stable subordinator density function, representing the density for random waiting times for the processes corresponding to the time-fractional diffusion equation (1.3.38). (Top right) Sample path of the subordinator (cumulative time)  $D(t)$ , the parent path, and the inverse subordinator (operational time)  $\tau(t)$  given by (1.3.33). Note that as  $t$  increases,  $\tau(t)$  need not advance. (Bottom left) Three sample paths of Brownian motion. (Bottom right) Three sample paths of Brownian motion with waiting times, constructed from the Brownian paths in the bottom left panel. The particles trace out the same Brownian paths in space, but now wait for potentially several time-steps at each location, as specified by the operation time  $\tau(t)$ . Source: Suzuki et al. (2023).

The probability density of Brownian motion with waiting times  $B_{\tau(t)}$  is governed by the time-fractional diffusion equation,

$${}^C_0 D_t^\beta u(x, t) = k^2 \Delta u(x, t), \tag{1.3.38}$$

$$u(x, t = 0) = u_0(x). \tag{1.3.39}$$

Here, the Caputo derivative is defined for  $0 < \beta < 1$  by

$${}^C_a D_t^\beta u(t) = \frac{1}{\Gamma(1 - \beta)} \int_a^t \frac{u'(s)}{|s - t|^\beta} ds. \tag{1.3.40}$$

For  $a = 0$ , this operator is characterized by the simple Laplace transform representation

$$\mathcal{L}[\mathcal{C}_0^{\beta} D_t^{\beta} u](s) = s^{\beta} \mathcal{L}[u](s) - s^{\beta-1} u(0). \quad (1.3.41)$$

Higher-order Caputo derivatives can be defined, although the Laplace transforms of the resulting operators involve initial conditions for derivatives of  $u$ ; see Section 2.3 of Meerschaert and Sikorskii (2011). The Caputo derivative is most frequently utilized as a derivative in time for initial-value problems, with the fractional order  $0 < \alpha < 1$ .

Before introducing the fundamental solution to the time-fractional diffusion, we introduce the Mittag-Leffler function (Mainardi et al., 2007; Mainardi, 2020)

$$E_{\theta}(z) = \sum_{\ell=0}^{\infty} \frac{z^{\ell}}{\Gamma(\theta \ell + 1)}, \quad \theta > 0. \quad (1.3.42)$$

This Mittag-Leffler function  $E_{\theta}(z)$  reduces to the exponential function  $e^z$  when  $\theta = 1$ , and has the following Laplace transform property

$$\mathcal{L}[E_{\theta}(-k^2 t^{\theta})](s) = \frac{s^{\theta-1}}{s^{\theta} + k^2}, \quad (1.3.43)$$

which immediately implies that  $E_{\beta}(-k^2 t^{\beta})$  solves the fractional ordinary differential equation

$$\mathcal{C}_0^{\beta} D_t^{\beta} u = k^2 u. \quad (1.3.44)$$

Returning to the diffusion equation (1.3.38) with initial condition  $u(x, t = 0) = \delta(x)$ , applying the Fourier transform in space implies that

$$\mathcal{F}[u(\cdot, t)](\xi) = E_{\beta}(-k^2 \xi^2 t^{\beta}), \quad (1.3.45)$$

which, as shown by Mainardi et al. (2007), yields a solution that can be written as

$$u(x, t) = t^{-\beta/2} U(|x|/t^{\beta/2}) \quad (1.3.46)$$

with

$$U(x) = \frac{1}{2} \sum_{k=0}^{\infty} \frac{(-x)^k}{k! \Gamma[-(\beta/2)k + 1 - (\beta/2)]} \quad (1.3.47)$$

being a special case of the Fox–Wright function. Note that  $U(x) = u(x, t = 1)$ . While the fundamental solution above is transcendental, it has the following properties: for  $\alpha = 1$ , it reduces to the solution (1.3.5) of the classical diffusion

equation; for  $0 < \alpha < 1$ , the solution decays faster than exponential and slower than Gaussian; and the second moment of the solution is

$$\sigma^2(t) = \frac{2}{\Gamma(\alpha + 1)} t^\beta. \quad (1.3.48)$$

Note that the  $t^\beta$  scaling of this second moment is consistent with the scaling of the fundamental solution above.

### 1.3.5 Continuous-Time Random Walks and Space-Time Fractional Diffusion

Both the  $\alpha$ -stable Lévy flight  $X_t^{\alpha,p}$ , which led to the space-fractional diffusion equation discussed in Section 1.3.3, and the Brownian motion with  $\beta$ -stable subordinator operational time  $B_{T^\beta(t)}$ , which led to the time-fractional diffusion equation discussed in Section 1.3.4, are examples of *continuous-time random walks*. A continuous-time random walk (CTRW) allows for a general family of processes in space to be time-changed by a general family of waiting-time processes. To illustrate this concept, we consider the process  $X_{T^\beta(t)}^{\alpha,p}$ , which is  $\alpha$ -stable Lévy flight  $X_t^{\alpha,p}$  defined at the discrete level by (1.3.29) time-changed by the  $\beta$ -stable subordinator process  $t \mapsto T^\beta(t)$  introduced in Section 1.3.4. This models a particle that performs independent jumps drawn from the  $\alpha$ -stable process, waiting at each point for a random time drawn independently from the  $\beta$ -stable subordinator process. As shown by, e.g., Meerschaert and Sikorskii (2011) (Section 4.5), the probability density of this particle position is then governed by a differential equation that is fractional in both time and space,

$$\begin{aligned} {}_0^C D_t^\beta u(x, t) &= \frac{-k^\alpha}{\cos(\pi\alpha/2)} \left[ p \left( {}_{-\infty}^{\text{RL}} D_x^\alpha u(x, t) \right) + (1 - p) \left( {}_x^{\text{RL}} D_\infty^\alpha u(x, t) \right) \right], \\ u(x, t = 0) &= u_0(x). \end{aligned} \quad (1.3.49)$$

While intuitive, this result deserves a more detailed discussion within the general theory of CTRWs. In the standard CTRW model, particles wait at a location for time drawn from a density function  $\psi$ , and jump to a new location by an increment drawn from a density function  $\phi$ . The waiting time and jump samples are assumed to be i.i.d., and uncoupled from each other (Zaburdaev et al., 2015; Metzler and Klafter, 2000; Scalas et al., 2004; Torrejon and Emelianenko, 2018). Thus, the densities  $\psi$  and  $\phi$  completely determine the CTRW. From the waiting time density  $\psi$ , the probability that a particle will remain at any given position for time  $t$  is

$$\Psi(t) = 1 - \int_0^t \psi(\tau) d\tau; \quad (1.3.50)$$

this is referred to as the *survival probability* of a CTRW particle. Then, given an initial probability density of a particle  $u_0(x) = u(x, t = 0)$ , which can also be thought of as an initial distribution of an ensemble of independent particles, the following equation was derived by Montroll and Weiss (1965) for the density at later time

$$u(x, t) = \Psi(t)u_0(x) - \int_0^t \psi(t - \tau) \int_{-\infty}^{\infty} \phi(y)u(x - y, \tau) dy d\tau. \quad (1.3.51)$$

This equation is central to the CTRW theory<sup>5</sup>. Taking the Laplace transform in time, the Fourier transform in space, and solving for  $\mathcal{F}[\mathcal{L}[u]](\xi, s)$  yields the Montroll–Weiss equation (Montroll and Weiss, 1965),

$$\mathcal{F}[\mathcal{L}[u]](\xi, s) = \frac{1 - \mathcal{L}[\psi](s)}{s} \frac{\mathcal{F}[u_0](\xi)}{1 - \mathcal{L}[\psi](s)\mathcal{F}[\phi](\xi)}. \quad (1.3.52)$$

If  $\phi$  is the  $\alpha$ -stable density (1.3.29) and  $\psi$  is the  $\beta$ -stable subordinator density (1.3.34), then  $\mathcal{F}[\phi]$  is given by the analytical formula (1.3.10) and  $\mathcal{L}[\psi]$  by (1.3.35), so that the Montroll–Weiss equation represents a closed-form solution of  $u$  in  $(\xi, s)$ -space. Unsurprisingly, it is impossible to perform inverse transforms and obtain  $u$  itself analytically, but  $u$  can be shown to satisfy (1.3.49) using the representations (1.3.41) and (1.3.26).

### 1.3.6 Lévy Walks and Fractional Material Derivatives

The superdiffusive  $\alpha$ -stable Lévy flight exhibits infinite mean-squared displacement (MSD), which is a drawback for certain applications. Related to this is the infinite speed of propagation intrinsic to Lévy flights, i.e., the fact that particles have a nonzero probability of traveling an arbitrary large distance in a unit of time. Brownian motion also suffers from this feature, although this probability of large excursions is so low that MSD remains finite. A prototypical model of the superdiffusion that cannot be described by a Lévy flight is ballistic motion, in which particles simply move from an initial configuration in fixed random directions with speed  $v$ , for all time  $t$ . A ballistic particle travels a distance  $vt$  in time  $t$  from an initial position  $x_0$ . If reorientations are allowed, then the positions of these so-called *sub-ballistic particles* in space-time are confined to a ballistic cone

<sup>5</sup> This equation was also derived by Scher and Lax (1973a,b) and is referred to as the CTRW equation of Scher and Lax by Klafter and Silbey (1980). Other authors, such as Torrejon and Emelianenko (2018) refer to this as the *master equation* of a CTRW.

$$\{(x, t) : x \in [x_0 - vt, x_0 + vt], t \geq 0\}. \tag{1.3.53}$$

Because the density function of the particle positions is compactly supported, all moments of the position are finite. Such a process cannot be described by Lévy flights.

To capture such a behavior, we introduce the *Lévy walk model*, following Zaburdaev et al. (2015). Such models are based on continuous-in-time motion of particles, rather than instantaneous jumps. A speed  $v$  of particles in a medium is specified; each particle moves with speed  $v$  in a chosen direction, before a reorientation event occurs, in which the direction changes instantaneously and the particle continues to move with speed  $v$  in the next direction. Assuming the direction at reorientation is sampled uniformly on the unit sphere, such a walk is determined by a PDF for the duration of movement  $\psi(\tau)$ . This leads to a survival probability  $\Psi(t)$  given by (1.3.50), with  $\psi$  now representing the duration density. Thus,  $\Psi(t)$  returns the probability that a particle has persisted in a given direction for time  $\tau$ , i.e., has *not* experienced reorientation for time  $\tau$ .

Similar to the CTRW case, a master equation can be derived for the probability density  $u(x, t)$  of the location of the particle in the Laplace–Fourier space:

$$\mathcal{F}[\mathcal{L}[u]](\xi, s) = \frac{\mathcal{L}[\Psi](s + iv\xi) + \mathcal{L}[\Psi](s - iv\xi)}{2 - \mathcal{L}[\psi](s + iv\xi) + \mathcal{L}[\psi](s - iv\xi)} \mathcal{F}[u_0](\xi). \tag{1.3.54}$$

Unlike the master equation for CTRWs, this equation exhibits coupling in Fourier and Laplace variables, representing coupling in space-time<sup>6</sup>. This results in governing equations that are considerably more complex than those of a standard CTRW. For a Lévy walk,  $\psi$  is taken to be a Pareto-type distribution,

$$\psi(\tau) = \frac{1}{\tau_0} \frac{\gamma}{(1 + \tau/\tau_0)^\gamma}, \quad \tau_0 > 0, \gamma > 0. \tag{1.3.55}$$

An asymptotic expansion of  $\mathcal{L}[\psi]$  and  $\mathcal{L}[\Psi]$  substituted in (1.3.54) yields the following approximation for the evolution of the density function of a Lévy walk in Fourier–Laplace space:

$$\mathcal{F}[\mathcal{L}[u]](\xi, s) \approx \frac{(s + iv\xi)^{\gamma-1} + (s - iv\xi)^{\gamma-1}}{(s + iv\xi)^\gamma + (s - iv\xi)^\gamma} \mathcal{F}[u_0](\xi). \tag{1.3.56}$$

Given  $v$  and  $u_0$ , this equation can be inverted to compute  $u(x, t)$ , but obtaining a governing equation in  $(x, t)$  is less straightforward from this point on, due

<sup>6</sup> A Lévy walk may be compared to a non-standard CTRW in which waiting times prior to jumps are correlated to the jump length, e.g., proportional to the jump length, so that long excursions are penalized by long waiting times, see Zaburdaev et al. (2015).

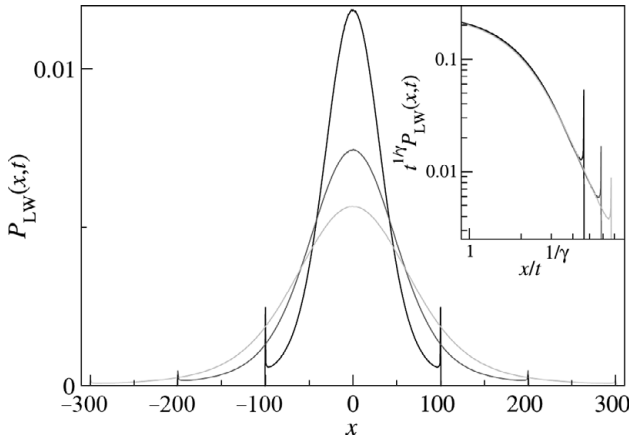


Figure 1.7 The evolution of PDF (denoted  $P_{LW}$  in the figure) of a Lévy walk, reproduced from (Zaburdaev et al., 2015). Here,  $\gamma = 3/2$  and the density is plotted for  $t = 100$  (black),  $t = 200$  (darker gray), and  $t = 300$  (lighter gray). The density mimics the density of a  $\gamma$ -stable Lévy flight in an interior region of the ballistic cone, scaling outwards as  $t^{1/\gamma}$ , supported inside the ballistic front (consisting of two points in one dimension) that scales outwards as  $t$ . Source: Suzuki et al. (2023).

to space-time coupling. Sokolov and Metzler (2003) suggested defining a fractional *material* or *substantial* derivative

$$(v^{-1} \partial_t \pm \partial_x)^{1/\gamma} u := \mathcal{F}^{-1} \mathcal{L}^{-1} [(s + iv\xi)^\gamma + (s - iv\xi)^\gamma \mathcal{F}[u_0](\xi)], \quad (1.3.57)$$

in order to obtain a governing equation for  $u(x, t)$ . Some works, such as those of Chen and Deng (2015), have explored numerical discretizations for these operators.

Despite the greater mathematical difficulties related to governing equations, as compared to other fractional models, Lévy walks have been widely used due to the physical nature of finite speed of propagation and finite MSD; see Zaburdaev et al. (2015) for a survey. When  $1 < \gamma < 2$ , by numerical approximations, it can be seen that  $u(x, t)$  evolves from a  $\delta$ -distribution with “a central part of the profile approximated by the Lévy distribution sandwiched between two ballistic peaks” that propagates at speed  $v$ , with an MSD and self-similarity property for large  $t$  that features a superdiffusive scale factor of  $t^{1/\gamma}$  (Zaburdaev et al., 2015), see Figure 1.7.

Finally, the comparison of normal diffusion, superdiffusion, and subdiffusion via MSD of the particle models and the scaling-in-time of the fundamental

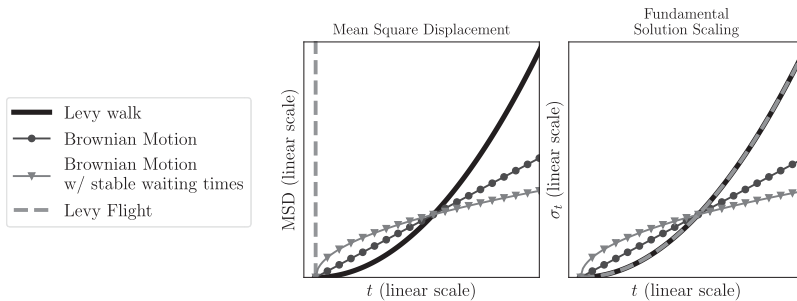


Figure 1.8 Brownian motion exhibits both MSD and scaling factor that are *linear* in time. Superdiffusive Lévy flight exhibits an infinite MSD and a fundamental solution scaling factor  $t^\alpha$  for  $\alpha > 1$ , while the superdiffusive Lévy walk exhibits the same scaling of the fundamental solution as well as a finite MSD that scales as  $t^\alpha$ . The subdiffusive Brownian motion with waiting times exhibits sublinear MSD and fundamental solution scaling, proportional to  $t^{1/\alpha}$  for  $\alpha < 1$ . Source: Suzuki et al. (2023).

solution to the diffusion equations governing the density functions are illustrated in Figure 1.8.

### 1.3.7 Fractional Brownian Motion

In Section 1.3.1, we introduced the standard diffusion model as an integer-order PDE that governs the PDF of a cloud of particles spreading around according to Brownian motion. In earlier sections, we learned that by generalizing the construction of such underlying microscopic motions to incorporate new anomalous effects (e.g., heavy-tailed jumps, stochastic waiting times, etc.), we could arrive at a generalizing time-/space-fractional PDE in each case, governing the PDF evolution of the underlying process, being either *subdiffusive* or *superdiffusive*.

Interestingly, it is possible to construct yet another class of important stochastic processes directly via Brownian motion without obtaining any fractional PDE in the limit, which alternatively can exhibit sub-super-diffusive behavior in the process. We will show that the corresponding PDF equation of such a process called *fractional Brownian motion* emerges as an *integer-order* PDE yet with a time-dependent diffusion coefficient.

#### Derivation of Fractional Brownian Motion

Fractional Brownian motion is the fractional derivative of a Brownian motion (Biagini et al., 2008; Meerschaert and Sikorskii, 2011). Suppose that  $B_t$  is a

standard Brownian motion, defined in Section 1.3.1, with the characteristic function

$$\mathbb{E}[e^{ikB_t}] = e^{-tk^2/2}, \forall t \geq 0.$$

The Caputo fractional derivative of order  $0 < \alpha < 1$  can be written in the form

$${}_{-\infty}^C D_x^\alpha f(x) = \frac{1}{\Gamma(1-\alpha)} \int_{-\infty}^x f'(u)(x-u)^{-\alpha} du.$$

We hope to be able to define the fractional Brownian motion by replacing  $f(x)$  by the Brownian motion  $B_t$ , but the derivative  $B'(s)$  does not even exist since the paths of a Brownian motion are nowhere differentiable (almost surely). However, for a continuous function  $g(s)$ , we can define

$$\int_a^b g(s)B(ds) \approx \sum_{i=1}^n g(s_i)B(\Delta s_i), \tag{1.3.58}$$

where

$$\Delta s = (b-a)/n, \quad s_j = a + j\Delta s, \quad B(\Delta s_j) = B(s_j) - B(s_{j-1}),$$

for  $j = 0, 1, \dots, n$ , and the approximating sum on the right converges (*in probability*) to the stochastic integral on the left as  $n \rightarrow \infty$ . Note that  $B(\Delta s_j)$  is normal with mean zero and variance  $s_j - s_{j-1}$ , and that  $B(\Delta s_1), \dots, B(\Delta s_n)$  are independent, since  $B_t$  has independent increments. Then  $\sum_j g(s_j)B(\Delta s_j)$  is normal with mean zero and variance  $\sum_j g^2(s_j)\Delta s$ , and it follows by taking the limit that

$$\int_a^b g(s)B(ds) \sim \mathcal{N}\left(0, \int_a^b |g(s)|^2 ds\right), \tag{1.3.59}$$

assuming that  $|g(s)|^2$  is integrable over  $a < s \leq b$ . As a common practice in mathematics, the improper integral is defined as a limit of proper integrals

$$\int_{-\infty}^b g(s)B(ds) = \lim_{a \rightarrow -\infty} \int_a^b g(s)B(ds) \quad \text{in probability,}$$

and then

$$\int_{-\infty}^b g(s)B(ds) \sim \mathcal{N}\left(0, \int_{-\infty}^b |g(s)|^2 ds\right), \tag{1.3.60}$$

assuming that  $|g(s)|^2$  is integrable over  $-\infty < s \leq b$ . Now we intend to define a *fractional derivative of the Brownian motion* by the formula

$$I(t) = \frac{1}{\Gamma(1-\alpha)} \int_{-\infty}^t (t-s)^{-\alpha} B(ds),$$

but the challenge is that since  $g(s) = (t - s)^{-\alpha}$ , we have

$$\int_{-\infty}^t |g(s)|^2 ds = \infty.$$

To work around this, we first define

$$I_a(t) = \frac{1}{\Gamma(1 - \alpha)} \int_a^t (t - s)^{-\alpha} B(ds)$$

and consider the difference

$$\begin{aligned} B_H(t) &= \lim_{a \rightarrow -\infty} I_a(t) - I_a(0) \\ &= \frac{1}{\Gamma(1 - \alpha)} \int_{-\infty}^{\infty} [(t - s)_+^{-\alpha} - (0 - s)_+^{-\alpha}] B(ds), \end{aligned} \tag{1.3.61}$$

where  $(x)_+ = x, \forall x > 0$  and vanishes otherwise. Here, we adopt the convention  $0^0 = 0$ .

**Remark 1.2** Since  $\int |g(s)|^2 ds < \infty$ ,  $g(s)$  being the integrand of the above stochastic integral, for any  $-1/2 < \alpha < 1/2$ , this above stochastic integral is defined only for this admissible range of  $\alpha \in (-1/2, 1/2)$ .

### Hurst Index H

The Hurst index  $H = 1/2 - \alpha$  for  $0 < H < 1$  governs the self-similarity of the fractional Brownian motion, defined in (1.3.61), that is,

$$B_H(ct) = c^H B_H(t). \tag{1.3.62}$$

To see why this is indeed the case, first note that the random (Brownian) measure  $B(ds)$  in (1.3.61) has a scaling property  $B(c ds) \sim c^{1/2} B(ds)$ , since for an interval  $V = [a, b]$ , we have

$$B(V) \sim \mathcal{N}(0, |V|)$$

and

$$B(cV) \sim \mathcal{N}(0, |cV|) \sim c^{1/2} B(V).$$

Then a change of variables  $s = cs'$  yields (1.3.62).

**Remark 1.3** (Special Case:  $H = 1/2$ ) The fractional Brownian motion  $B_H(t)$  is a Brownian motion  $B_t$  on  $t \in \mathbb{R}$  when  $H = 1/2$ . Indeed since in the special case  $H = 1/2$ , we have  $\alpha = 0$ , and then for  $t \geq 0$ , we get

$$B_H(t) = \int_{-\infty}^{\infty} I(0 \leq s < t) B(ds) = B_t - B_0 = B_t,$$

while for  $t < 0$  we get

$$B_H(t) = \int_{-\infty}^{\infty} I(t \leq s < 0) B(ds) = B_0 - B_t = -B_1(t) \sim B_t.$$

It follows from self-similarity  $B_H(ct) \sim c^H B_H(t)$  that a fractional Brownian motion satisfies  $B_H(t) \sim t^H B_H(1), \forall t \in \mathbb{R}$ , where the stochastic integral  $B_H(1)$  is normal with mean zero.

**The PDF of Fractional Brownian Motion**

The PDF  $p(x, t)$  of a fractional Brownian motion  $B_H(t)$  satisfies a diffusion equation with variable coefficients

$$\frac{\partial}{\partial t} p(x, t) = (2HDt^{2H-1}) \frac{\partial^2}{\partial x^2} p(x, t), \quad \forall t > 0, \tag{1.3.63}$$

where the case  $1/2 < H < 1$  is associated with a *superdiffusive* process, and  $0 < H < 1/2$  represents a *subdiffusive* fractional Brownian motion. In fact, (1.3.63) is an *integer-order* diffusion model with time-variable diffusivity  $2HDt^{2H-1}$ , which grows nonlinearly with time (except when  $H = 1$ ).

To see why (1.3.63) holds, we note that  $B_H(t)$  has a PDF  $p(x, t)$  with Fourier transform

$$\hat{p}(k, t) = \mathbb{E}[e^{-ikB_H(t)}] = e^{-Dt^{2H}k^2}, \quad \forall t > 0,$$

for some constant  $D > 0$ . Then, by taking the first time-derivative on both sides we have

$$\frac{d}{dt} \hat{p}(k, t) = 2HDt^{2H-1} (ik)^2 \hat{p}(k, t),$$

where its inverse Fourier transform yields (1.3.63).

The increments of the fractional Brownian motion are *not* independent; however, its increments are *stationary*, i.e.,

$$B_H(t_2) - B_H(t_1) \sim B_H(t_2 - t_1).$$

Moreover, the fractional Brownian motion  $B_H(t)$  with  $H \neq 1/2$  is *not* a Lévy process, since it does not have independent increments. There are many Gaussian stochastic processes whose PDFs solve (1.3.63); however, fractional Brownian motion is *the only self-similar Gaussian process with stationary increments*.

**Fractal Sample Paths and Covariance Structure of  $B_H(t)$**

The sample path of a fractional Brownian motion  $B_H(t)$  is a random fractal with dimension  $d = 2 - H$  (Falconer, 2003, Theorem 16.7). As the Hurst index

$H$  increases from  $1/2$  to  $1$ , we are applying a fractional integral of increasing order, so the path of  $B_H(t)$  becomes smoother. Moreover, the covariance structure of a fractional Brownian motion  $B_H(t)$  is given by

$$\mathbb{E}[B_H(t)B_H(s)] = \frac{C}{2} \left[ |t|^{2H} + |s|^{2H} - |t-s|^{2H} \right]. \tag{1.3.64}$$

This can be easily computed employing two important properties of  $B_H(t)$ , the self-similarity and stationary increments. When  $0 < s < t$ , since  $B_H(t) \sim t^H B_H(1)$ , we have  $\mathbb{E}[B_H(t)^2] = t^{2H} C$ , where  $C = \mathbb{E}[B_H(1)^2]$ . Now one can write

$$(B_H(t) - B_H(s))^2 = B_H(t)^2 + B_H(s)^2 - 2B_H(t)B_H(s),$$

and take expectations to get

$$C(t-s)^{2H} = Ct^{2H} + Cs^{2H} - 2\mathbb{E}[B_H(t)B_H(s)].$$

That yields

$$\mathbb{E}[B_H(t)B_H(s)] = \frac{C}{2} \left[ t^{2H} + s^{2H} - (t-s)^{2H} \right].$$

The case  $0 < t < s$  is similar, and we can combine these two cases to obtain (1.3.64). Note that the case for  $t < 0$  or  $s < 0$  is again similar, and leads to the same result.

### 1.3.8 Tempered Fractional Calculus

Consider a CTRW with independent power-law jumps each having probability density function

$$f(x) = C \alpha x^{-\alpha-1} \mathbf{1}_{[C^{1/\alpha}, \infty)}(x).$$

The second moment of such distribution is divergent that accounts for the anomalous jumps, called *Lévy flights*. We learned that the limit of this sum is an  $\alpha$ -stable Lévy motion, whose probability density  $p(t, x)$  satisfies the fractional diffusion

$$\frac{\partial p(t, x)}{\partial t} = k^2 \frac{\partial^\alpha p(t, x)}{\partial x^\alpha}$$

with diffusion coefficient  $k^2$ . In practice, however, many physical processes take place in *bounded domains* in *finite times* and have *finite moments*. Therefore, the divergent second moments may not be applicable to such processes. There exist different techniques to address this barrier (Sokolov et al., 2004; Mantegna and Stanley, 1994), among which the most popular one is a new variation of the fractional calculus, where power-laws are *tempered*

Table 1.2. *Tempered fractional derivatives of order  $\alpha \in (0, 1]$ ,  $\lambda \geq 0$  and  $x \in [a, b]$ .*

	Left-Sided, ${}_a^*D_x^{\alpha,\lambda} f(x), x \geq a$	Right-Sided, ${}_x^*D_b^{\alpha,\lambda} f(x), x \leq b$
C	$\frac{e^{-\lambda x}}{\Gamma(1-\alpha)} \int_a^x (x-s)^{-\alpha} \frac{d e^{\lambda s} f(s)}{ds} ds$	$\frac{e^{\lambda x}}{\Gamma(1-\alpha)} \int_x^b (x-s)^{-\alpha} \frac{d e^{-\lambda s} f(s)}{ds} ds$
RL	$\frac{e^{-\lambda x}}{\Gamma(1-\alpha)} \frac{d}{dx} \int_a^x (x-s)^{-\alpha} e^{\lambda s} f(s) ds$	$\frac{e^{\lambda x}}{\Gamma(1-\alpha)} \frac{d}{dx} \int_x^b (x-s)^{-\alpha} e^{-\lambda s} f(s) ds$

by an exponential factor (Sabzikar et al., 2015; Baeumer and Meerschaert, 2010; Cartea and del Castillo-Negrete, 2007; Beghin, 2015; Wu et al., 2016; Liemert et al., 2017; Boniece et al., 2018). This exponential tempering has both mathematical and practical advantages (Sabzikar et al., 2015; Beghin, 2015, and references therein). Tempered fractional diffusion applies an exponential tempering factor to the particle jump density, i.e.,

$$f_\epsilon(x) = C_\epsilon^{-1} x^{-\alpha-1} e^{\lambda x} \mathbf{1}_{[\epsilon,\infty)}(x),$$

where

$$C_\epsilon = \int_\epsilon^\infty x^{-\alpha-1} e^{\lambda x} dx.$$

Theorems 2.1 and 2.2 in Sabzikar et al. (2015) prove that a CTRW with tempered density and an independent Poisson process  $N_t^\epsilon$  converges to a tempered stable Lévy motion, whose probability density  $p(t, x)$  is the point source solution to the tempered space-fractional diffusion equation

$$\frac{\partial p(t, x)}{\partial t} = \mp k^2 \frac{\partial^{\alpha,\lambda} p(t, x)}{\partial x^\alpha} \tag{1.3.65}$$

(‘−’ is for  $0 < \alpha < 1$  and ‘+’ is for  $1 < \alpha < 2$ ). This equation models transient superdiffusion, where a particle plume initially spreads faster than what the traditional diffusion equation predicts, but later relaxes to a typical diffusion profile, see Sabzikar et al. (2015) for more details. The corresponding tempered fractional derivatives of order  $\alpha$  with tempering parameter  $\lambda \geq 0$  in Caputo and Riemann–Liouville sense are given in Table 1.2.

### 1.3.9 Variable-Order Fractional Derivatives

Given the physical meaning within stochastic models of the fractional order  $\alpha$  in derivatives such as (1.3.17), (1.3.24), and (1.3.40), it is reasonable to expect that these parameters may vary in space and/or time. Variable-order fractional models are convenient to describe anomalous diffusion in the case

of heterogeneous materials or media, or, more generally, when the nature of the diffusion process (subdiffusive, superdiffusive, and classical) changes with space and/or time. While models with constant fractional order are the simplest and most widely used, some of the model descriptions we have discussed are enriched by the use of variable fractional orders as *field variables*.

More flexible models, characterized by variable fractional orders, have been introduced for both space- and time-fractional differential operators (Razminia et al., 2012; Antil and Rautenberg, 2019; Zheng and Wang, 2020b; Darve et al., 2021; D’Elia and Glusa, 2021) and several discretization methods have been designed (Schneider et al., 2010; Chen et al., 2015; Zheng and Wang, 2020a). The improved descriptive power of variable-order fractional operators has been demonstrated in some recent works on parameter estimation (Pang et al., 2019, 2020a; Zheng et al., 2020).

Given a function

$$\alpha : \mathbb{R}^d \times \mathbb{R}^+ \rightarrow \mathbb{R}, \tag{1.3.66}$$

i.e., a function  $\alpha(\mathbf{x}, t)$  of space and time, we define variable-order operators as follows. For a function  $u(\mathbf{x}, t)$  with  $\mathbf{x} \in \mathbb{R}^d$  and  $t \in \mathbb{R}$ , we define the variable-order fractional Laplacian<sup>7</sup> as

$$\mathcal{L}^{\alpha(\cdot, \cdot)} u(\mathbf{x}, t) = C_{d, \alpha(\mathbf{x}, t)} \text{p.v.} \int_{\mathbb{R}^d} \frac{u(\mathbf{x}, t) - u(\mathbf{y}, t)}{|\mathbf{x} - \mathbf{y}|^{d + \alpha(\mathbf{x}, t)}} d\mathbf{y}. \tag{1.3.67}$$

Here,  $\alpha(\mathbf{x}, t)$  is restricted to take values in  $(0, 2)$ . Note that for constant  $\alpha$ ,  $\mathcal{L}^\alpha = (-\Delta)^{\alpha/2}$ . For  $d = 1$  and  $\alpha(x, t)$  restricted to  $(0, 1)$ , we define the variable-order left-sided Riemann–Liouville fractional derivative as

$${}_{-\infty}^{\text{RL}} D_t^{\alpha(\cdot, \cdot)} u(x, t) = \frac{1}{\Gamma(1 - \alpha(x, t))} \frac{\partial}{\partial x} \int_{-\infty}^x \frac{u(y, t)}{|x - y|^{\alpha(x, t)}} dy. \tag{1.3.68}$$

The right-sided Riemann–Liouville may be defined for variable order in an analogous way. We define the variable-order Caputo fractional derivative, again for  $\alpha(x, t)$  taking values in  $(0, 1)$ , as

$${}_{-\infty}^{\text{C}} D_t^{\alpha(\cdot, \cdot)} u(x, t) = \frac{1}{\Gamma(1 - \alpha(x, t))} \int_{-\infty}^t \frac{\partial u}{\partial t}(x, s) \frac{1}{|s - t|^{\alpha(x, t)}} ds. \tag{1.3.69}$$

### 1.3.10 Distributed-Order Fractional Calculus

There are physical systems that demonstrate a non-scaling behavior corresponding to crossover between different power-laws or even non-power-law

<sup>7</sup> For more recent works and novel definitions of variable-order fractional Laplacians, we refer the reader to Antil and Rautenberg (2019) and D’Elia and Glusa (2021).

behavior. Distributed-order models offer a tool for mathematical modeling of such *multi-scale* phenomena. In this case, the differential order is distributed over a range of values rather than being just a fixed fraction as it is in fractional operators. Caputo (1995, 2001) proposed the use of distributed-order fractional derivatives to generalize the stress–strain relation of inelastic media and Fick’s law. The connection of such operators in subdiffusion with the corresponding CTRW was first established in Chechkin et al. (2002), where the authors proposed diffusion-like equations with time and space fractional derivatives of distributed-order for the kinetic description of anomalous diffusion and relaxation phenomena. They studied the “natural form” of the corresponding distributed-order diffusion equation, which describes an underlying random process that may lead to retarded subdiffusion (super slow diffusion) or accelerating superdiffusion. Later, in Chechkin et al. (2008), they discussed the “modified form” of distributed-order equations with both temporal and spatial fractional derivatives and showed the process describing anomalous relaxation and diffusion phenomena getting less anomalous in the course of time evolution (accelerating subdiffusion and decelerating superdiffusion). For more detailed discussions see also Chechkin et al. (2003); Umarov and Steinberg (2006); Kochubei (2008); Chen and Kumagai (2008); Kochubei (2011); Jiao et al. (2012); Sandev et al. (2015, 2018) and the references therein. The application of distributed-order fractional derivatives is also discussed in rheological models (Lorenzo and Hartley, 2002; Atanackovic et al., 2009), economic processes with distributed memory fading (Tarasova and Tarasov, 2018), time domain analysis of control, filtering and signal processing (Li et al., 2011; Li and Chen, 2014), vibration and optimal control (Zaky and Machado, 2017; Duan and Baleanu, 2018), and frequency domain analysis (Bagley and Torvik, 2000). There is also a rapidly growing interest in the use of distributed-order fractional derivatives in the construction of mathematical models in the field of uncertainty quantification as the inherent uncertainty of experimental data can be directly incorporated into the differential operators (Kharazmi et al., 2017). The distributed-order fractional derivative over  $x \in [a, b]$  with order  $\alpha \in [\alpha_{min}, \alpha_{max}]$  can be expressed in the general form as

$${}^D\mathcal{D}_\phi u(x) = \int_{\alpha_{min}}^{\alpha_{max}} \phi(\alpha) {}^*D_x^\alpha u(x) d\alpha, \quad \forall x > a, \quad (1.3.70)$$

in which the prescript  $*$  stands for any type of fractional derivative, and  $\phi(\alpha)$  can be thought of as a distribution function, where  $\alpha \mapsto \phi(\alpha)$  is a continuous mapping in  $[\alpha_{min}, \alpha_{max}]$ . We note that  $\alpha_{min}$  and  $\alpha_{max}$  are only the theoretical lower and upper terminals in the definition of distributed-order derivatives. However, in general, the distribution function  $\phi(\alpha)$  can arbitrarily

confine the domain of integration in each realization of practical problems, and thus requires different regularity of underlying function space. In Kharazmi et al. (2017), the authors defined the *distributed fractional Sobolev space* on  $\mathbb{R}$ , denoted by  ${}^\phi\mathcal{H}(\mathbb{R})$ , as a compliant underlying function space for the distributed-order derivatives. Let  $\phi \in L^1([\alpha_{\min}, \alpha_{\max}])$ ,  $0 \leq \alpha_{\min} < \alpha_{\max}$ , be non-negative. Then,

$${}^\phi\mathcal{H}(\mathbb{R}) = \left\{ v \in L^2(\mathbb{R}) : \int_{\alpha_{\min}}^{\alpha_{\max}} [\phi(\alpha)(1 + |\omega|^2)^\alpha]^{\frac{1}{2}} \mathcal{F}(v)(\omega) d\alpha \in L^2(\mathbb{R}) \right\}, \quad (1.3.71)$$

endowed with norm

$$\| \cdot \|_{\phi, I} = \inf_{\tilde{v} \in {}^\phi\mathcal{H}(\mathbb{R}), \tilde{v}|_I = (\cdot)} \| \tilde{v} \|_{\phi, \mathbb{R}}.$$

Subsequently, the *distributed fractional Sobolev space* on the finite closed interval  $I$ , denoted by  ${}^\phi\mathcal{H}(I)$ , is defined as

$${}^\phi\mathcal{H}(I) = \{ v \in L^2(I) : \exists \tilde{v} \in {}^\phi\mathcal{H}(\mathbb{R}) \text{ s.t. } \tilde{v}|_I = v \},$$

equipped with the equivalent left- and right-sided norms

$$\| \cdot \|_{l, \phi, I}^2 = \| \cdot \|_{L^2(I)}^2 + \int_{\alpha_{\min}}^{\alpha_{\max}} \phi(\alpha) \| {}_{x_L}^{RL}D_x^\alpha(\cdot) \|_{L^2(I)}^2 d\alpha, \quad (1.3.72)$$

$$\| \cdot \|_{r, \phi, I}^2 = \| \cdot \|_{L^2(I)}^2 + \int_{\alpha_{\min}}^{\alpha_{\max}} \phi(\alpha) \| {}_x^{RL}D_{x_R}^\alpha(\cdot) \|_{L^2(I)}^2 d\alpha. \quad (1.3.73)$$

We note that when  $\phi > 0$  is continuous in  $I$ ,  ${}^\phi\mathcal{H}(\mathbb{R})$  is equivalent to  $H^{\alpha_{\max}}(\mathbb{R})$ . However, in general, the choice of  $\phi$  can arbitrarily confine the domain of integration in practice. In other words,  $\alpha_{\min}$  and  $\alpha_{\max}$  are only the theoretical lower and upper terminals in the definition of distributed-order fractional derivatives. For instance, in a distributed subdiffusion problem, the temporal derivative is associated with  $\alpha_{\min} = 0$  and  $\alpha_{\max} = 1$ , and in a superdiffusion problem, the theoretical upper terminal  $\alpha_{\max} = 2$ . We particularly can define  $\phi$  in any possible subset of the interval  $[\alpha_{\min}, \alpha_{\max}]$ . Hence, in each realization of a physical process (e.g., sub- or superdiffusion)  $\phi$  can be obtained from data, where the theoretical setting of the problem remains invariant yet requiring the solution to have less regularity (since  ${}^\phi\mathcal{H}(\mathbb{R}) \supset H^{\alpha_{\max}}(\mathbb{R})$  in general, see Figure 1.9).

### 1.3.11 Fractional Vector Calculus

The history of fractional vector calculus (FVC) is not as long as fractional calculus (Adda, 1998; Engheta, 1998; Naqvi and Abbas, 2004; Meerschaert

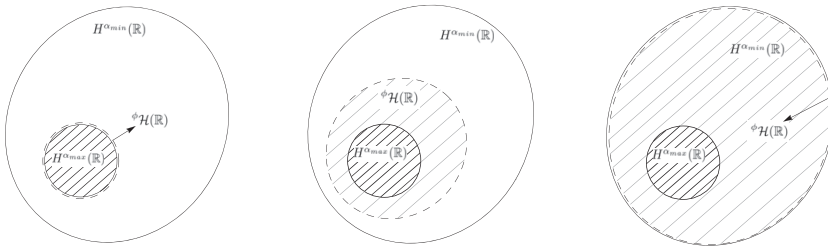


Figure 1.9 Schematic of distributed fractional Sobolev space  $\phi\mathcal{H}(\mathbb{R})$ : (left)  $\phi = \delta(\alpha - \alpha_{max})$  hence  $\phi\mathcal{H}(\mathbb{R}) = H^{\alpha_{max}}(\mathbb{R})$ ; (middle)  $\phi$  defined on a compact support in  $[\alpha_{min}, \alpha_{max}]$ , hence,  $\phi\mathcal{H}(\mathbb{R}) \supset H^{\alpha_{max}}(\mathbb{R})$ ; (right)  $\phi = \delta(\alpha - \alpha_{min})$ , where  $\phi\mathcal{H}(\mathbb{R}) = H^{\alpha_{min}}(\mathbb{R})$ . Here  $\delta$  represents the Dirac delta function/distribution. Source: Kharazmi et al. (2017). Copyright ©2017 Society for Industrial and Applied Mathematics. Reprinted with permission. All rights reserved.

et al., 2006). Some of the main approaches in formulating FVC have been briefly described in Tarasov (2008). In particular, we review the two major contributions by Meerschaert et al. (2006) and Tarasov (2008).

• **Meerschaert et al.’s Approach:** In this approach (Meerschaert et al., 2006), the fractional integral operator is defined in a general form as

$$\mathcal{J}_M^{1-\beta}[\cdot] = \int_{\|\theta\|=1} \theta D_\theta^{\beta-1} \theta^T[\cdot] M(d\theta), \quad \theta \in \mathbb{R}^d, \tag{1.3.74}$$

where  $D_\theta^{\beta-1}(\cdot)$  denotes the inverse Fourier transform of  $(i\mathbf{k} \cdot \theta)^{\beta-1} \mathcal{F}[\cdot]$ ,  $0 < \beta \leq 1$ , the symbol  $\theta^T$  denotes transpose of column vector  $\theta$ , and  $M(d\theta)$  represents a positive finite-measure on the set of unit vectors. Given the integral operator (1.3.74), the fractional gradient, fractional divergence, and fractional curl operators are defined as follows

$$\nabla_M^\beta u(\mathbf{x}) = \mathcal{J}_M^{1-\beta} \nabla u(\mathbf{x}) = \int_{\|\theta\|=1} \theta D_\theta^\beta u(\mathbf{x}) M(d\theta), \tag{1.3.75}$$

$$\text{div}_M^\beta \mathbf{V}(\mathbf{x}) = \nabla \cdot \mathcal{J}_M^{1-\beta} \mathbf{V}(\mathbf{x}) = \int_{\|\theta\|=1} D_\theta^\beta \mathbf{V}(\mathbf{x}) \cdot \theta M(d\theta), \tag{1.3.76}$$

$$\text{curl}_M^\beta \mathbf{V}(\mathbf{x}) = \nabla \times \mathcal{J}_M^{1-\beta} \mathbf{V}(\mathbf{x}) = \int_{\|\theta\|=1} \nabla \times \theta D_\theta^{\beta-1} \theta \cdot \mathbf{V}(\mathbf{x}) M(d\theta), \tag{1.3.77}$$

where the operation symbols  $\cdot$  and  $\times$  denote inner and outer products of two vectors, respectively, and  $D_\theta^\beta \mathbf{V}(\mathbf{x})$  represents the component-wise directional fractional derivative for vector field  $\mathbf{V}$ .

Note that in the case of vector field  $\mathbf{V}(\mathbf{x})$ , the fractional integration operator  $\mathcal{J}_M^{1-\beta}$  transforms the original field to another field  $\mathbf{V}^\tau = \mathcal{J}_M^{1-\beta} \mathbf{V}$  in a nonlocal fashion. Therefore, the classical divergence and curl theorems for the resulting vector field  $\mathbf{V}^\tau$  will yield the fractional counterparts for the vector field  $\mathbf{V}$  after substituting  $\mathbf{V}^\tau = \mathcal{J}_M^{1-\beta} \mathbf{V}$ . This is, however, a point of controversy as discussed in the following.

• **Tarasov’s Approach:** In Tarasov (2008), Tarasov argued that although Meerschaert et al.’s approach (Meerschaert et al., 2006) allows the use of usual (integer) integral Stokes’ and Green’s theorems, it cannot be considered as a fractional generalization of vector calculus as the proposed curl operator can be presented as the usual (integer) curl operator. In return, he proposed to replace the Riemann–Liouville derivative with the Caputo one to overcome the failure of the Newton–Leibniz formula for the fractional generalization of Green’s formula. Thus, he proved the *fundamental theorem of fractional calculus (FTFC)* by considering the fractional Riemann–Liouville integral and Caputo derivative as its antiderivative operator. Recall  ${}_a\mathcal{I}_x^\alpha$  and  ${}_a^C D_x^\alpha$  being the fractional integral and Caputo derivative operators, respectively, which act on a real-valued function  $f(x) \in L_1[a, b]$  for  $\alpha > 0$ , and  $f(x) \in AC^n[a, b]$  for  $n - 1 < \alpha < n$ . Here  $AC^n[a, b]$  stands for the space of functions with absolutely continuous  $n$ -th derivatives in  $[a, b]$ . Then, FTFC can be represented as

$${}_a^C D_x^\alpha {}_a\mathcal{I}_x^\alpha f(x'') = f(x), \quad (\alpha > 0),$$

$${}_a\mathcal{I}_x^\alpha {}_a^C D_x^\alpha f(x'') = f(x) - f(a), \quad (0 < \alpha < 1),$$

which implies that the Caputo derivative of the fractional integral of a function returns the function itself when the orders of derivative and integral are the same. Thus, the Caputo derivative is the corresponding antiderivative operator of the fractional integral.

Let  $W$  be a domain of  $\mathbb{R}^3$ . Let  $f(\mathbf{x})$  and  $F(\mathbf{x})$  be real-valued scalar and vector fields, respectively, that have continuous derivatives up to order  $n - 1$  on  $W$ , such that the  $n - 1$  derivatives are absolutely continuous, i.e.,  $f, F \in AC^n[W]$ . Then, a fractional generalization of the nabla operator is defined by

$$\nabla_W^\alpha = {}^C \mathbf{D}_W^\alpha = \mathbf{e}_1 {}^C D_W^\alpha[x] + \mathbf{e}_2 {}^C D_W^\alpha[y] + \mathbf{e}_3 {}^C D_W^\alpha[z], \quad n - 1 < \alpha < n,$$

and hence, the fractional gradient, divergence, and curl operators are defined as

$$\text{Grad}_W^\alpha f = {}^C \mathbf{D}_W^\alpha f = \mathbf{e}_l {}^C D_W^\alpha [x_l] f(x, y, z), \quad (1.3.78)$$

$$\text{Div}_W^\alpha F = ({}^C \mathbf{D}_W^\alpha, F) = {}^C D_W^\alpha [x_l] F_l(x, y, z), \quad (1.3.79)$$

$$\text{Curl}_W^\alpha F = [{}^C \mathbf{D}_W^\alpha, F] = \mathbf{e}_l \varepsilon_{lmk} {}^C D_W^\alpha [x_m] F_k(x, y, z), \quad (1.3.80)$$

respectively, using Einstein's notation and  $\varepsilon_{lmk}$  as Levi-Civita symbol. Other relations for fractional differential and integral vector operations, such as

$$\text{Div}_W^\alpha \text{Grad}_W^\alpha = ({}^C \mathbf{D}_W^\alpha)^2 = {}^C D_W^\alpha [x_l] {}^C D_W^\alpha [x_l], \quad (1.3.81)$$

and fractional circulation, flux, and volume integral are given in Tarasov (2008). The extension to fractional Green's theorem for a rectangle, fractional Stokes' theorem, and fractional Gauss' theorem for a parallelepiped are also proved in Tarasov (2008).

## 1.4 Global vs. Local Numerical Methods

Computational approaches appear as suitable tools for solving FODEs/FPDEs since exact solutions are only available for a small class of linear problems in unbounded domains. Here, we do not aim to provide a complete description of all existing numerical methods. We rather define the two main classes of computational approaches extensively employed for solving fractional-order problems in the present book: (i) *hp*-methods, including spectral methods (also known as *p*-methods) and spectral element methods (also known as *hp*-methods), and (ii) finite-difference methods.

In *hp*-methods, instead of solving the strong (original) form of the fractional model, we discretize the corresponding weak (variational) form of the problem. Such a weak form is obtained by multiplying the governing equation by another proper function, called *test function*, integrating over the computational domain, and then using integration-by-parts to transfer the derivative load from the solution to test function. After the weak/variational form is derived, we represent/approximate the solution in terms of a finite linear combination of some particular functions, called *basis/trial functions*. By plugging the solution expansion into the weak form and testing the problem on as many as the number of expansion terms, a linear system for the corresponding unknown solution coefficients is constructed. In spectral methods (*p*-methods), the basis/test functions are nontrivially defined over the whole computational domain and the whole domain is treated as a single element. Moreover in spectral methods, the numerical solution converges to the true solution by increasing the number of terms in the basis expansion (i.e., increasing the maximum basis order in the solution expansion). In spectral

element methods (*hp*-method), we partition the domain into a finite number of non-overlapping patches, called *elements*, over which the basis/test functions are locally defined. In the formulation of spectral element methods, the degree of bases in each element can arbitrarily change such that the method can be understood as a spectral method-like in each element. Therefore, the solution in a spectral element method converges to the exact solution as the number of elements and/or the number of expansion terms (i.e., the basis order) in each element increases. The proper mathematical type of the convergence will be later rigorously determined.

In the finite-difference methods, however, we approximate the solution of a fractional model at certain temporal/spatial grid points, and then, we satisfy the governing equation at each of those grid points, replacing all the underlying fractional derivatives in the governing equation (i.e., the strong form) with their finite-difference approximations. This gives a finite system of algebraic equations to be solved in place of the corresponding differential equation. Therefore, the numerical solution converges point-wise to the true solution by increasing the number of grid points in space and/or time.

**Remark 1.4** Given the aforementioned descriptions, finite-difference methods are “local” discretization schemes intrinsically; however, the nature of spectral and spectral element methods is indeed “global (*nonlocal*)” as the true solution is always approximated via basis *functions* (rather than grid *points*) over the entire global domain/sub-domains.

### Why Global Numerical Methods?

The local finite-difference schemes are generally easy to implement; however, such numerical methods impose history/nonlocal calculations in the context of FODEs/FPDEs, which contain multiple summations over the solution history or spatial neighborhood. Hence, they can be computationally expensive as the inherent memory-dependent/nonlocal nature of fractional operators increases the complexity of arithmetic operations. Hence, such global *hp*-methods naturally fit the nonlocal processes, described by FODEs/FPDEs.

To address the aforementioned computational challenges, this book introduces the spectral theories on fractional and tempered fractional Sturm–Liouville problems in both regular and singular forms. The corresponding eigenfunctions and their generalizations will establish new classes of orthogonal basis/test functions with attractive spectral properties, which make them suitable for constructing efficient spectral and spectral element methods for fractional-order problems. Moreover, recalling the Askey scheme of orthog-

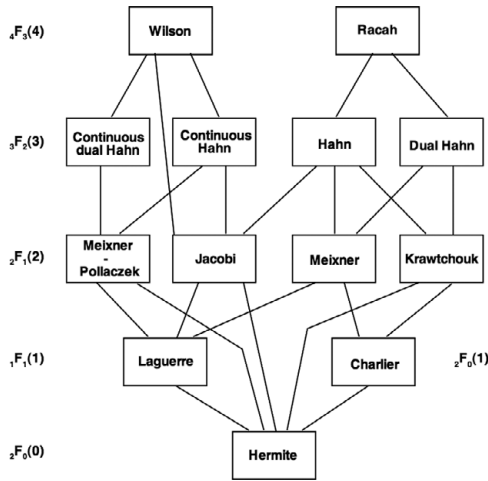


Figure 1.10 The Askey scheme of classical orthogonal polynomials. This big family of orthogonal polynomials is only a subset of the new extended family of poly-fractionals and can be recovered for the special case of fractional order  $\nu = 2$ . Source: Xiu and Karniadakis (2002). Copyright ©2002 Society for Industrial and Applied Mathematics. Reprinted with permission. All rights reserved.

onal polynomials, shown in Figure 1.10, such an extension from Jacobi polynomials of integer order to their fractional order, introduced in Chapter 2, will create new families of orthogonal functions that can be used as basis functions to represent solutions of FODEs and FPDEs, encoding the nonlocal processes with heavy-tail measures.

Nonetheless, the time-integration of nonlinear and/or stiff FPDEs, where the characteristic time scales of problems strongly vary, will be inevitably treated by finite-difference methods. In Chapter 7, we will introduce the generalization of the well-known multi-step implicit-explicit (IMEX) methods in addition to the fast and accurate computation of the corresponding history terms for carrying out stable long-time integrations.